

This document is confidential and is proprietary to the American Chemical Society and its authors. Do not copy or disclose without written permission. If you have received this item in error, notify the sender and delete all copies.

Driving Forces of Protein Diffusion

Journal:	<i>The Journal of Physical Chemistry Letters</i>
Manuscript ID	jz-2020-03006b.R2
Manuscript Type:	Letter
Date Submitted by the Author:	n/a
Complete List of Authors:	Mostajabi Sarhangi, Setare; Arizona State University, School of Molecular Sciences Matyushov, Dmitry; Arizona State University, School of Molecular Sciences

SCHOLARONE™
Manuscripts

Driving Forces of Protein Diffusion

Setare Mostajabi Sarhangi and Dmitry V. Matyushov*

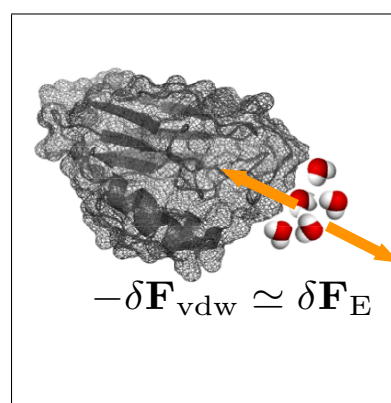
Department of Physics and School of Molecular Sciences, Arizona State University, PO Box 871504, Tempe, AZ 85287-1504

E-mail: dmitrym@asu.edu, Tel:(480)965-0057

Abstract

Diffusivity of a protein (a Brownian particle) is caused by random molecular collisions in the Stokes-Einstein picture. Alternatively, it can be viewed as driven by unbalanced stochastic forces acting from water on the protein. Molecular dynamics simulations of protein mutants carrying different charges are analyzed here in terms of the van der Waals (vdW) and electrostatic forces acting on the protein. They turn out to be remarkably strongly correlated and the total force is largely a compensation between vdW and electrostatic forces. Both vdW and electrostatic forces relax on the same time scale of 5-6 ns separated by six orders of magnitude from the relaxation time of the total force. Similar phenomenology applies to the dynamics and statistics of the fluctuating torque responsible for rotational diffusion. Standard linear theories of dielectric friction are grossly inapplicable to translational and rotational diffusion of proteins overestimating friction by many orders of magnitude.

TOC Graphic



1
2
3 Protein diffusion is mostly viewed as a hydrodynamic boundary-value problem for an object of
4 complex shape moving through a liquid.¹⁻³ Physical complications to this simplified picture have
5 been realized in terms of water forming a sufficiently dense hydration shell traveling together with
6 the protein. The hydrodynamic (Stokes) radius of the protein thus mostly exceeds either the van der
7 Waals (vdW) or the gyration radius.⁴⁻⁶ However, this generic picture does not address the question
8 of what are the physical driving forces that cause the translational and rotational Brownian diffusion
9 of a protein. Hydrodynamic arguments assume that there is no difference between diffusion of
10 a protein and of any colloidal particle of similar size. We show here that this view is incorrect
11 and there are very specific properties of the protein and its interface with the water shell which
12 determine the statistics and dynamics of random forces kicking the protein into random translations
13 and rotations.
14

15 The idea that motion of charged molecules through polar liquids cannot be reduced to hydro-
16 dynamics was offered by a number of classical papers on dielectric friction. Initial studies of the
17 problem, linked to the names of Onsager⁷ and Zwanzig,⁸ established the main principle: a delayed
18 response of the liquid dipoles to a moving charge leads to dielectric loss responsible for additional
19 friction. These linear theories, and theoretical formulations that followed,⁹⁻¹¹ assumed that the
20 hydrodynamic, ζ_a^H , and dielectric, ζ_a^D , friction components are additive in the overall friction co-
21 efficient $\zeta_a = \zeta_a^H + \zeta_a^D$ entering the diffusion coefficient through the Einstein equation
22

23

$$D_a = k_B T / \zeta_a \quad (1)$$

24
25 It applies to both translational ($a = t$) and rotational ($a = r$) diffusion.
26

27 For translational diffusion of a spherical ion, these theories predict that ζ_t^D scales linearly with
28 the squared charge Q and inversely with the cube of the ionic radius R_0
29

30

$$\zeta_t^D \propto (Q^2 / R_0^3) \tau_D \quad (2)$$

31 The relaxation time of the liquid dipoles τ_D entering this equation is associated with the time of
32

dielectric relaxation of the medium (Debye relaxation time), which is about 9 ps for water at room temperature. However, more careful considerations^{11,12} show that the relaxation time entering ζ_t^D is close to the longitudinal dielectric time¹³ $\tau_L = (\epsilon_\infty/\epsilon_s)\tau_D \simeq 0.2$ ps, which is much shorter than τ_D due to the ratio of the high-frequency, ϵ_∞ (close to the squared refractive index n_D^2), and static, ϵ_s , dielectric constants of water. If these parameters are used with the common radius of the globular protein, $R_0 \simeq 1.5 - 2$ nm, dielectric friction becomes negligible compared to the Stokes drag and one returns to the realm of standard hydrodynamics applied to the friction coefficient in eq 1.

Translational friction can be given a more microscopic meaning in terms of random microscopic forces acting on the protein.⁹ When translations are described by the overdamped Langevin equation with no memory effects (assumption implicit in eq 1), the translational friction coefficient is given as the time integral of the force-force time correlation function^{9,11,12}

$$\zeta_t = (\beta/3) \int_0^\infty dt \langle \delta\mathbf{F}(t) \cdot \delta\mathbf{F}(0) \rangle \quad (3)$$

where $\mathbf{F}(t)$ is the total force acting on the particle, $\delta\mathbf{F} = \mathbf{F} - \langle \mathbf{F} \rangle$, and $\beta = (k_B T)^{-1}$.

The assumption of friction additivity, adopted in essentially all classical work on dielectric friction,^{7-9,14} implies statistical independence (no statistical correlations) of the “hydrodynamic” and electrostatic, \mathbf{F}_E , forces contributing to the total force \mathbf{F} acting from water on the protein

$$\mathbf{F} = \mathbf{F}_{\text{vdw}} + \mathbf{F}_E \quad (4)$$

The “hydrodynamic” force, which should not be confused with the physical hydrodynamic force produced by the liquid flux,¹⁵ is not well defined as a physical force. This label is used to designate random collisions of the surrounding molecules with the target molecule leading to the standard Einstein-Stokes diffusivity.¹⁶ This somewhat vague language is not needed in the framework of eq 3 since one can ask what are the physical forces making the protein diffuse. This is the question addressed in this study.

The separation in eq 4 puts all non-electrostatic forces between a target particle and the surrounding medium into the component \mathbf{F}_{vdw} . In force fields employed in molecular dynamics (MD) simulations of proteins discussed below, non-electrostatic forces are associated with van der Waals (vdW) interactions modeled by site-site Lennard-Jones (LJ) potentials. Based on this physical assignment, \mathbf{F}_{vdw} is used in eq 4 to specify the “hydrodynamic” force.

The goal of this study is to critically examine the physical forces contributing to friction experienced by proteins in water and the possibility that electrostatics still plays a significant role in protein diffusivity, despite the arguments presented above. The assumption of statistical independence between \mathbf{F}_{vdw} and \mathbf{F}_E was put under question for simple electrolyte ions in a number of previous studies.^{12,17–20} The question of potential statistical correlations between different forces affecting diffusivity becomes even more critical for proteins given that viscoelastic shape fluctuations are strongly coupled for these molecules with polarization of their hydration shells.^{21–24} Charged residues are located at the surface of the protein and any elastic alteration of the protein shape leads to a density fluctuation of its hydration shell and to a corresponding electrostatic fluctuation of the protein-water interface.²⁵ Our simulations presented here confirm strong statistical correlations between \mathbf{F}_{vdw} and \mathbf{F}_E , which become a major prominent feature of protein diffusivity.

An additional support in favor of the importance of electrostatics in protein diffusivity comes from dynamic considerations. The electrostatic component of friction follows directly from eq 3 by using $\mathbf{F}_E = Q\mathbf{E}_w$ for the electrostatic force

$$\zeta_t^D = \frac{\beta Q^2}{3} \tau_E \langle (\delta \mathbf{E}_w)^2 \rangle \quad (5)$$

Here, $\mathbf{E}_w = Q^{-1} \sum_i q_i \mathbf{E}_i$ is the average electric field of water acting on the protein charges q_i and τ_E is the relaxation time of \mathbf{E}_w .

Equation 5 separates the total charge from the overall electrostatic force acting from water on the charges in the protein, $\mathbf{F}_E = \sum_i q_i \mathbf{E}_i$. There are at least two advantages to this formulation. First, analytical theories of dielectric friction are formulated in terms of electric fields produced by

1
2
3 the polarized medium inside the solute.⁸ Second, the electric field of water inside the protein is often
4 rather uniform,²⁶ and, in contrast to the force, can be measured through calibrated shifts of optical
5 and vibrational lines.²⁷ When $Q = 0$, the nonzero electrostatic force reported by simulations comes
6 from the superposition of field inhomogeneities inside the protein. Correspondingly, the total vdW
7 force comes from adding all LJ potentials ϕ_{kj}^{LJ} between the water molecules k and atoms j of the
8 protein, $\mathbf{F}_{\text{vdW}} = -\nabla \sum_{k,j} \phi_{kj}^{\text{LJ}}$.

9
10
11
12
13
14
15
16
17
18
19
20
21
22
23
24
25
26
27
28
29
30
31
32
33
34
35
36
37
38
39
40
30
41
42
43
44
45
46
47
48
49
50
51
52
53
54
55
56
57
58
59
60
Solvated proteins demonstrate a significant breadth of field fluctuations²⁶ expressed in terms
of the field variance $\sigma_E^2 = \langle (\delta \mathbf{E}_w)^2 \rangle$ in eq 5. Even more importantly, the relaxation time τ_E of
the electric field of the water shell produced inside the protein in the range of 5 – 16 ns.²⁶ This
amounts a retardation factor of at least 10^4 compared to the dielectric longitudinal relaxation time
 τ_L anticipated by dielectric theories. These estimates of σ_E^2 and τ_E would make ζ_t^D the dominant
contribution to translational friction (see discussion below and Figure S7). However, the results
presented here show that this expectation is not realized because the additivity between vdW and
electrostatic friction assumed in the standard models^{7–9,14} and in deriving eq 5 breaks down dra-
matically. Protein diffusivity turns out to be more complex than anticipated.

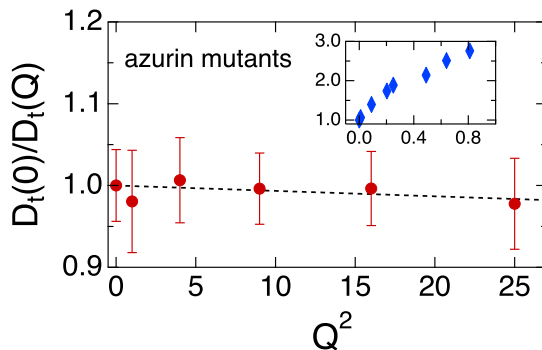


Figure 1: $D_t(0)/D_t(Q)$ vs Q^2 for the mutants of azurin. Points refer to MD simulations and the dashed line is a linear fit through the points. The error bars are obtained from 10 MD trajectories for each mutant. The inset shows $D_t(0)/D_t(Q)$ vs Q^2 for small LJ ions (fractional charge used in MD simulations).¹²

These arguments raise the question of whether any, even empirical, indication of the effect of
electrostatics on diffusivity can be put forward. One such prediction of dielectric theories is the

dependence of the translational diffusion coefficient $D_t(Q)$ on the solute charge Q . According to dielectric theories based on eq 5,^{7,8,14} one anticipates a linear scaling with Q^2

$$\frac{D_t(0)}{D_t(Q)} = 1 + AQ^2 \quad (6)$$

where the constant A depends on specific values of the hydrodynamic and dielectric friction coefficients and on cross-correlations between vdW and electrostatic forces. Figure 1 shows the results of our simulations for $D_t(Q)$ of six mutants of the protein azurin carrying zero and negative charges in the range $Q = 0, \dots, -5$ (Figure 2). The mutants were created by protonating/deprotonating the surface ionizable residues and by changing the oxidation state of the protein between oxidized ($Q = -2$) and reduced ($Q = -3$) states. Since the active site of azurin is relatively close to the protein surface ($\simeq 8 \text{ \AA}$), all mutations affect the distribution of charge close to the protein-water interface (see Supporting Information (SI) for more details and the simulation protocol).

The translational diffusion coefficients in Figure 1 were calculated by integrating the time correlation function of the center of mass velocity $\mathbf{v}_c(t)$

$$D_t = \frac{1}{3} \int_0^\infty dt C_v(t), \quad C_v(t) = \langle \mathbf{v}_c(t) \cdot \mathbf{v}_c(0) \rangle \quad (7)$$

For each charge mutant, 10 short trajectories (1 ns) were produced by choosing starting configurations along a single long trajectory. The average diffusion coefficients are shown by points and the bars ($\simeq 5\%$) indicate standard deviations. No dependence of the diffusion coefficient on the protein charge is seen within the simulation uncertainties. The analysis of the experimental database for protein translational diffusivity has shown that the standard Stokes-Einstein equation (eq 1) holds within 20% deviation limits.²⁸ The effects of charge variation caused by pH and ion association are expected to fall within $\pm 20\%$ limits. Further, capillary zone electrophoresis of protein charge ladders²⁹ has shown protein ionic mobilities linear in charge, $\mu \propto Q$. Curvatures observed at low electrolyte concentrations have been explained within standard models of colloidal mobility.³⁰

The Einstein equation is the result of the Markovian approximation for the random forces acting

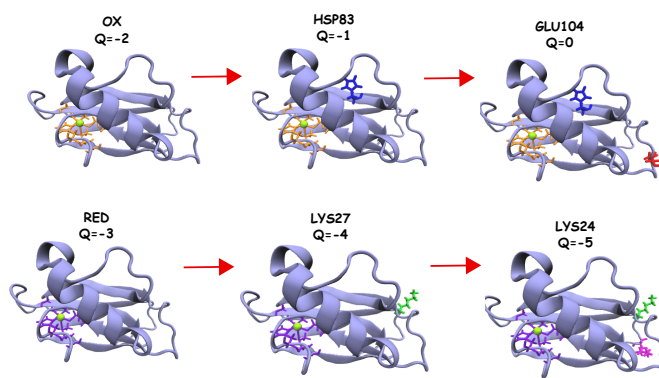


Figure 2: Azurine mutants created by altering the charge of ionizable surface residues and the oxidation state of the active site. The surface residues are color-coded according to the following rule: histidine (blue), glutamate (red), lysine-24 (green) and lysine-27 (magenta); Cu of the active site is rendered green, orange (Ox) and purple (Red) colors of the active site are used to specify the oxidation state.

on the protein, which makes the friction coefficient ζ a constant parameter. Random forces generally carry memory, requiring a time-dependent memory function $\zeta(\tau)$ convoluted with fluctuating velocity in the generalized Langevin equation.³¹ If $\zeta(\tau) = \zeta(0)m(\tau)$ is given by the product of the initial amplitude $\zeta(0)$ and a quickly decaying memory function $m(\tau)$ ($m(0) = 1$), the diffusion coefficient can be represented in terms of the force variance³² (see SI)

$$D_t(Q) = 3 [\beta^2 \langle (\delta \mathbf{F})^2 \rangle \tau_m]^{-1} \quad (8)$$

where $\tau_m = \int_0^\infty d\tau m(\tau)$ is the integrated memory time.

The variance of the total force and of its vdW and electrostatic components in eq 8 are shown in Figure 3a. Fluctuations of the electrostatic and vdW forces make comparable contributions to the overall force variance. There is also a cross term, $\langle \delta \mathbf{F}_{\text{vdw}} \cdot \delta \mathbf{F}_E \rangle$, which contributes to the variance with a factor of two

$$\langle (\delta \mathbf{F})^2 \rangle = \sigma_{\text{vdw}}^2 + \sigma_E^2 + 2\sigma_{\text{vdw},E}, \quad \sigma_{\text{vdw},E} = \langle \delta \mathbf{F}_{\text{vdw}} \cdot \delta \mathbf{F}_E \rangle \quad (9)$$

The cross term is negative in magnitude, but its negative turns out to be remarkably close to the

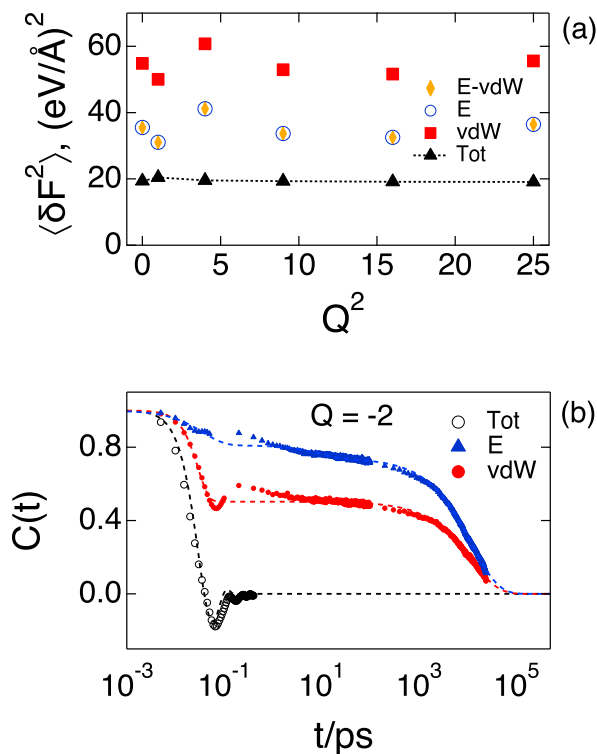


Figure 3: (a) Variance of the total force (Tot) acting from water on azurin $\langle (\delta\mathbf{F})^2 \rangle$ and its electrostatic (E) and vdW components vs Q^2 . “E-vdw”, nearly coinciding with “E”, refers to the negative of the cross-correlation between electrostatic and vdW forces ($-\sigma_{\text{vdw},\text{E}}$, eq 9). The dotted line connects the points for the total force. (b) Force-force time correlation function for the vdW, electrostatic, and total force acting from water on azurin carrying the charge $Q = -2$. The dashed lines are fits to analytical functions presented in the SI.

positive variance of the electrostatic force

$$-\langle \delta \mathbf{F}_E \cdot \delta \mathbf{F}_{\text{vdw}} \rangle \simeq \langle (\delta \mathbf{F}_E)^2 \rangle \quad (10)$$

(circles and diamonds are nearly indistinguishable on the plot scale in Figure 3a, see Table S4 for the actual values). As a result, the total force variance is given, with good accuracy, as

$$\langle (\delta \mathbf{F})^2 \rangle \simeq \langle (\delta \mathbf{F}_{\text{vdw}})^2 \rangle - \langle (\delta \mathbf{F}_E)^2 \rangle \quad (11)$$

The total force variance also turns out to be nearly independent of the protein charge (closed triangles in Figure 3a). Turning to eq 8, this result implies that neither the force variance nor the relaxation time τ_m show any significant dependence on Q for the diffusion coefficients shown in Figure 1. This result is quite distinct from a substantial effect of charge on diffusivity of simple LJ ions:¹² adding a single charge lowers the diffusion coefficient of an iodide-size ion by a factor of $\simeq 3$ (inset in Figure 1). Ionic diffusivity is suppressed by a combination of an increased force variance and retarded dynamics.

The remarkable near equality between $-\langle \delta \mathbf{F}_E \cdot \delta \mathbf{F}_{\text{vdw}} \rangle$ and $\langle (\delta \mathbf{F}_E)^2 \rangle$ implies that fluctuations of the electrostatic and vdW forces are driven by the same collective motion. The mode capable of producing such highly correlated fluctuations is the elastic deformation of the protein synchronously moving both the surface charges and the water molecules in the hydration shell. A similar near equality between the cross term and the electrostatic force variance was observed by Kumar and Maroncelli³³ for a rigid dipolar diatomic solute, with dimensions of iodine, in polar liquids. However, this exact compensation does not occur for small spherical ions in water.¹² This distinction points to the importance of the coupling between the internal motions (rotating dipole in Kumar-Maroncelli case³³ and elastic deformations of the protein here) and the polar medium.

The mechanism of protein elastic deformations, leading to eq 10, is supported by comparing the dynamics of electrostatic and vdW fluctuations on the one hand to the dynamics of the total force on the other hand. The total force decays, through oscillations, on the time scale of $\simeq 0.01$ ps

(see Table S5 and Figure S5), while the relaxation times for the vdW and electrostatic components are on the time scale of 5 – 6 ns (note the logarithmic time scale in Figure 3b, also see Table S5). The relaxation times for the total force and for its components are separated by six orders of magnitude. The nearly parallel time traces of the long-time tails of the electrostatic and vdW force-force correlation functions echo the result for the static limit, pointing again to their common origin. The decay of correlations for the vdW force is always faster than for the electrostatic correlations because of a higher amplitude of the initial ballistic decay (Figure S4).

It is important to stress that the strong separation of characteristic time scales for the total force and for the component forces is amenable to measurement: transport properties, such as diffusion, are affected by the total force while many time-resolved spectroscopic techniques report the electric field dynamics.¹¹ Specifically, a near constancy of $\langle(\delta\mathbf{F}_E)^2\rangle$ vs Q (Figure 3a) implies that the variance of the electric field $\langle(\delta\mathbf{E}_w)^2\rangle$ produced by water decays as Q^{-2} with the protein charge. Fluctuations of the electric field contribute to inhomogeneous broadening $\Delta\omega$ of spectral lines of optical and vibrational probes placed inside the protein.^{27,34} These line shapes are predicted to become narrower, $\Delta\omega \propto Q^{-1}$, as the charge of the protein deviates from the isoelectric point. A number of proteins,³⁵ in particular green fluorescence proteins,³⁶ can be brought to the state of high charge when these predictions can potentially be tested.

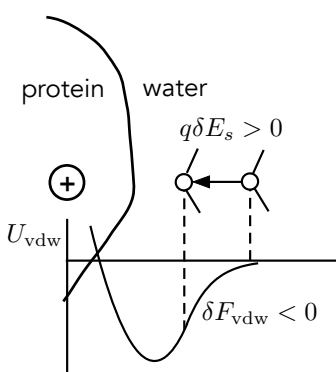


Figure 4: Diagram explaining negative cross-correlations between vdW and electrostatic forces (see text).

The reason for a negative cross correlation between vdW and electrostatic forces is illustrated in Figure 4. Charges of ionized surface residues orient water dipoles along the local electric field.

Such polarization of the surface waters leads to a positive field at the positive ion and a negative field at the negative ion (projected on the axis connecting the ion with the water molecule, Figure 4). An elastic fluctuation bringing a water molecule closer to the protein creates $\delta F_{\text{vdw}} < 0$ and $\delta F_E = q\delta E_s > 0$, thus producing a negative cross-correlation. The vdW force has an opposite sign on the repulsion branch of the LJ potential, but, because of a longer range of attractions, there are more water molecules residing within the attraction part of the interaction potential.

The arguments leading to eq 5 for the dielectric friction experienced by a moving ion can be equally applied to solute's rotations.^{8,37} If one assumes that the field \mathbf{E}_w is approximately uniform within the protein (an assumption confirmed by simulations²⁶), the torque acting on the protein through electrostatic interactions becomes

$$\mathbf{T}_E(t) = \mathbf{M}_0(t) \times \mathbf{E}_w(t) \quad (12)$$

where $\mathbf{M}_0(t)$ is the fluctuating protein dipole. Fluctuations (or, alternatively, delayed response⁸) of this torque lead to dissipation through dielectric rotational friction entering the rotational diffusion coefficient D_r (see SI for the derivation)

$$(2D_r)^{-1} = (2D_r^0)^{-1} + \frac{(\beta M_0)^2}{6} \tau_E \langle (\delta \mathbf{E}_w)^2 \rangle \quad (13)$$

where D_r^0 is the hydrodynamic rotational diffusion coefficient.

The value of D_r is given by the time integral of the correlation function of the angular velocity, similar to eq 7. Alternatively, it can be calculated from the relaxation time of the unit vector $\hat{\mathbf{u}}(t)$ specifying the protein orientation^{2,38,39}

$$D_r = (2\tau_r)^{-1}, \quad \tau_r = \int_0^\infty dt C_r(t) \quad (14)$$

1
2
3 where the orientational autocorrelation function is (Figure S6)
4
5
6

7 $C_r(t) = \langle \hat{\mathbf{u}}(t) \cdot \hat{\mathbf{u}}(0) \rangle$ (15)
8
9

10 This algorithm was used in the analysis of our simulations identifying $\hat{\mathbf{u}}(t)$ with the protein dipole
11 moment $\hat{\mathbf{u}}(t) = \mathbf{M}_0(t)/M_0(t)$.
12
13

14 When the parameters relevant to a solvated protein (azurin here) are entered to eq 13, the di-
15 electric friction term exceeds the hydrodynamic term by six-seven orders of magnitude (Figure
16 S7). The value of translational friction is overestimated by about the same magnitude if eq 5 is
17 applied. The standard linear theories of dielectric friction affecting either translational or rotational
18 diffusion are grossly inapplicable to protein mobility.
19
20
21
22
23

24 The actual rotational times calculated from simulations (from 30 to 100 ns depending on Q ,
25 Table S6) fall in the range roughly consistent with the hydrodynamic value¹¹ $\tau_r^0 = (2D_r^0)^{-1} \simeq$
26 $4\pi\beta R_0^3\eta = 9$ ns estimated at $R_0 \simeq 1.44$ nm (calculated with McVol code⁴⁰), where η is water's
27 viscosity. The effect of electrostatic forces is expected to be much more severe according to eq
28 13. This disconnect between expectations of standard theories and MD results points to what could
29 already be anticipated from the analysis of forces: a strong statistical correlation between vdW
30 and electrostatic torques, leading to the breakdown of the standard recipe for evaluating the rota-
31 tional dielectric friction.⁸ Indeed, the dynamics of the total torque and of its electrostatic component
32 follow the general phenomenology observed for the forces: the total torque decays, through oscil-
33 lations, with the effective relaxation time of $\simeq 0.01$ ps (Figure 5), while the electrostatic torque
34 decays much slower, with the effective relaxation time of $\simeq 1 - 4$ ns. These conclusions are made
35 from calculations of the torque-torque autocorrelation function $C_T(t)$ shown in Figures 5 and S9
36
37
38
39
40
41
42
43
44
45
46
47

48 $C_T(t) = \langle \mathbf{T}(t) \cdot \mathbf{T}(0) \rangle$ (16)
49
50
51
52
53
54
55
56
57
58
59
60

59 where the total torque $\mathbf{T}(t)$ is imposed by the water shell on the protein. In contrast, the electrostatic
60 torque $\mathbf{T}_E(t)$ is calculated from eq 12, in which both the protein dipole and the water electric field

1
2
3
4
5
6
7
8
9
10
11
12
13
14
15
16
17
18
19
20
21
22
23
24
25
26
27
28
29
30
31
32
33
34
35
36
37
38
39
40
41
42
43
44
45
46
47
48
49
50
51
52
53
54
55
56
57
58
59
60
are fluctuating variables.

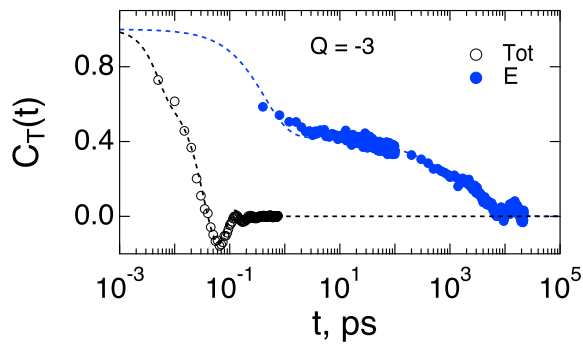


Figure 5: Normalized torque-torque time autocorrelation function (eq 16) for the electrostatic (E, eq 12) and total (Tot) torque acting from water on azurin carrying the charge $Q = -3$. The dashed lines are fits to analytical functions discussed in the SI. The average relaxation times are 1.3 ns (E) and 0.017 ps (Tot).

Instead of eqs 5 and 13, stressing the importance of dielectric friction, we find that the standard Stokes-Einstein-Debye (SED) prescription for the ratio D_t/D_r approximately holds (Figure 6)

$$D_t/(R_0^2 D_r) = 4/3 \quad (17)$$

Even though the hydrodynamic ratio is approximately satisfied, there are still substantial deviations of translational and rotational diffusion coefficients from hydrodynamic predictions: a factor 3 – 4 smaller for D_t (Figure S8) and a factor 4-6 smaller for D_r (Table S6) when compared to the corresponding hydrodynamic results. These differences mostly cancel out in the ratio shown in Figure 6. Note, however, that the difference in scaling with the protein radius between translational, $D_t \propto R_0^{-1}$, and rotational, $D_r \propto R_0^{-3}$, diffusion coefficients does not allow to adjust the hydrodynamic radius to fit both D_t and D_r . On a more fundamental level, the balance between the vdW and electrostatic forces and torques found here indicates that no such simple fix should exist: the electrostatic forces are affected by the total charge of the protein (except for $Q = 0$), while the electrostatic torque is mostly affected by the protein dipole.

The results shown in Figure 6 allow us to make two conclusions. First, no essential dependence on the protein charge found for translational diffusion is likely applicable to rotational diffusion as

well. Accurate calculations of rotational diffusion are harder to achieve by MD simulations because of much longer time scales involved. This limitation is likely responsible for the scatter in Figure 6. Second, there is no reason to assume the translation-rotation decoupling⁴¹ for proteins in solution as reported in crowded environments⁴² and in confinement.⁴³

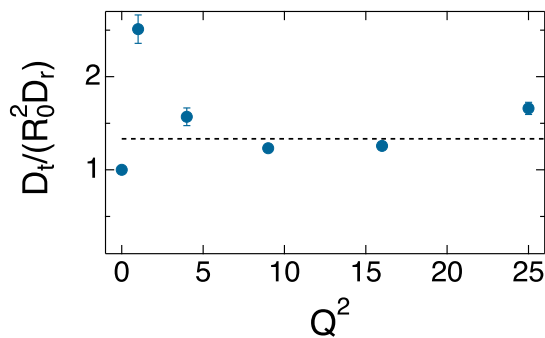


Figure 6: $D_t / (R_0^2 D_r)$ vs Q^2 for mutants of azurin, $R_0 = 1.44$ nm is the effective radius of the protein. The dashed line indicates the prediction of the SED equation, eq 17. The error bars are based on the data shown in Figure 1 (some are smaller than the point size).

The traditional view of Stokes-Einstein diffusion of colloidal particles¹⁶ suggests that diffusivity is caused by random collisions of the liquid molecules with the (Brownian) particle. Even though restated in many textbooks, this picture is inaccurate. Single-molecule collisions are not possible in dense liquids and one has to view diffusivity as caused by collective excitations of the liquid producing disbalances in forces acting from the liquid on different sides of the particle. The universal and more short-ranged vdW interactions are expected to produce forces and torques acting on the particle surface. Their disbalances are caused by uncompensated density fluctuations of the liquid on different side of the particle, in contrast to individual collisions. The electrostatic component of the force depends on how close the charges are to the interface. In this regard, many colloidal particles are stabilized in solution by surface solvation, due to charges located close to the polar liquid. In that case as well, collective fluctuations of both density and dipolar orientations of polar molecules in the interface, mostly uncorrelated on different sides of the particle, will produce random forces moving the colloidal particle. In this scenario, both vdW and electrostatic forces are driven by fluctuations in the interface and should affect the diffusivity of both large and small

1
2
3 particles. The force disbalance is related to the ratio of the correlation length of the corresponding
4 force to the particle size.
5
6

7 The solvated protein studied here gives a perfect illustration of this general picture. The more
8 short-ranged vdW forces between the water shell and the surface residues produce fluctuations
9 $\delta\mathbf{F}_{\text{vdW}}$ caused by density fluctuations of the water molecules closest to the protein surface. The
10 action of electrostatic forces on the protein charges is more long-ranged, as evidenced by the slow
11 convergence of the corresponding variances calculated as functions of the thickness of the water
12 shells.⁴⁴ For fluctuations of the electric field, leading to $\delta\mathbf{F}_E$, saturation occurs within the water
13 shell of $\simeq 10 \text{ \AA}$ from a protein or a peptide.⁴⁴ Fluctuations of the electric field involve many liquid
14 molecules and the picture of single-molecule collisions is clearly inapplicable here.
15
16

17 From eq 9 one finds that the total force variance is reduced by electrostatic interactions to about
18 40% of the vdW force
19
20

$$\langle(\delta\mathbf{F})^2\rangle \simeq 0.4\langle(\delta\mathbf{F}_{\text{vdW}})^2\rangle \quad (18)$$

21 The details of the dynamical and statistical correlation between the vdW and electrostatic forces
22 and torques are highly specific of the protein-water interface. Particularly noteworthy is the slow
23 relaxation time, in the range 4–15 ns, for both the vdW and electrostatic forces acting on the protein
24 (Table S5). In the case of electrostatic forces, this amounts to a retardation factor of four orders of
25 magnitude compared to longitudinal dielectric relaxation commonly associated with electrostatic
26 forces as indeed found in simulations of simple ions.¹²
27
28

29 A strong correlation between electrostatic and vdW forces dramatically reduces the electrostatic
30 friction which, according to linear dielectric models,^{7–9,14} is predicted to slow down both the rota-
31 tional and translational diffusion by many orders of magnitude. This prediction does not hold, but
32 there is still a substantial slowing down of both translational and rotational diffusivity by a factor of
33 3–6 compared to hydrodynamic estimates. The delicate balance between vdW and electrostatic
34 forces found here can be affected by conformational flexibility of the protein, implying that the
35 diffusion coefficient should fluctuate on the time-scale of conformational motions not because of
36 the altered shape, but more so because of the altered balance of forces. The same arguments apply
37
38

1
2
3 to any change of conditions which shift the balance of forces. Along these lines, any changes that
4 make proteins stiffer (e.g., through the substrate binding) are expected to reduce diffusivity.
5
6
7
8
9

10 Supporting Information Available 11

12
13 Simulation protocol, derivation of equations for the dielectric friction affecting translations and
14 rotations, and the analysis of time correlation functions from MD simulations.
15
16
17
18

19 Notes 20

21
22 The authors declare no competing financial interests.
23
24
25
26

27 Acknowledgement 28

29
30 This research was supported by the National Science Foundation (CHE-1800243) and through
31 XSEDE resources (TG-MCB080071).
32
33
34
35

36 References 37

38
39 (1) Brune, D.; Kim, S. Predicting protein diffusion coefficients. *Proc. Natl. Acad. Sci. USA* **1993**,
40 *90*, 3835–3839.
41
42 (2) Smith, P. E.; van Gunsteren, W. F. Translational and rotational diffusion of proteins. *J. Mol.*
43 *Biol.* **1994**, *236*, 629–636.
44
45 (3) Grimaldo, M.; Roosen-Runge, F.; Zhang, F.; Schreiber, F.; Seydel, T. Dynamics of proteins
46 in solution. *Quart. Rev. Biophys.* **2019**, *52*, e7.
47
48 (4) Choy, W.-Y.; Mulder, F. A. A.; Crowhurst, K. A.; Muhandiram, D. R.; Millett, I. S.; Do-
49 niach, S.; Forman-Kay, J. D.; Kay, L. E. Distribution of molecular size within an unfolded
50
51
52
53
54
55
56
57
58
59
60

1
2
3 state ensemble using small-angle X-ray scattering and pulse field gradient NMR techniques.
4
5 *J. Molec. Biol.* **2002**, *316*, 101–112.
6
7

8 (5) Nygaard, M.; Kragelund, B. B.; Papaleo, E.; Lindorff-Larsen, K. An efficient method for
9 estimating the hydrodynamic radius of disordered protein conformations. *Biophys. J.* **2017**,
10 *113*, 550–557.
11
12 (6) Grisham, D. R.; Nanda, V. Hydrodynamic radius coincides with the slip plane position in the
13 electrokinetic behavior of lysozyme. *Proteins* **2018**, *86*, 515–523.
14
15 (7) Hubbard, J.; Onsager, L. Dielectric dispersion and dielectric friction in electrolyte solutions.
16 *I. J. Chem. Phys.* **1977**, *67*, 4850–4857.
17
18 (8) Nee, T. W.; R. Zwanzig, R. Theory of dielectric relaxation in polar liquids. *J. Chem. Phys.*
19 **1970**, *52*, 6353–6363.
20
21 (9) Wolynes, P. Dynamics of electrolyte solutions. *Ann. Rev. Phys. Chem.* **1980**, *31*, 345–376.
22
23 (10) Bagchi, B.; Biswas, R. Ionic mobility and ultrafast solvation: Control of a slow phenomenon
24 by fast dynamics. *Acc. Chem. Res.* **1998**, *31*, 181–187.
25
26 (11) Bagchi, B. *Molecular relaxation in liquids*; Oxford University Press: Oxford, 2012.
27
28 (12) Samanta, T.; Matyushov, D. V. Mobility of large ions in water. *J. Chem. Phys.* **2020**, *153*,
29 044503.
30
31 (13) Kivelson, D.; Friedman, H. Longitudinal dielectric relaxation. *J. Phys. Chem.* **1989**, *93*, 7026–
32 7031.
33
34 (14) Zwanzig, R. Dielectric friction on a moving ion. II. Revised theory. *J. Chem. Phys.* **1970**, *52*,
35 3625–3628.
36
37 (15) Dhont, J. K. G. *An Introduction to dynamics of colloids*; Studies in interface science; Elsevier
38 Science, 1996; Vol. 2.
39
40
41
42
43
44
45
46
47
48
49
50
51
52
53
54
55
56
57
58
59
60

1
2
3 (16) Einstein, A. *Investigations on the theory of the Brownian movement*; BN Publishing, 2011.
4
5 (17) Berkowitz, M.; Wan, W. The limiting ionic conductivity of Na^+ and Cl^- ions in aqueous
6 solutions: Molecular dynamics simulation. *J. Chem. Phys.* **1987**, *86*, 376–382.
7
8 (18) Koneshan, S.; Rasaiah, J. C.; Lynden-Bell, R. M.; Lee, S. H. Solvent structure, dynamics, and
9 ion mobility in aqueous solutions at 25°C. *J. Phys. Chem. B* **1998**, *102*, 4193–4204.
10
11 (19) Chong, S. H.; Hirata, F. Dynamics of solvated ion in polar liquids: An interaction-site-model
12 description. *J. Chem. Phys.* **1998**, *108*, 7339–7349.
13
14 (20) Rasaiah, J. C.; Lynden-Bell, R. M. Computer simulation studies of the structure and dynamics
15 of ions and non-polar solutes in water. *Phil. Trans. R. Soc. A* **2001**, *359*, 1545–1574.
16
17 (21) Halle, B.; Nilsson, L. Does the dynamic Stokes shift report on slow protein dynamics? *J.*
18 *Phys. Chem. B* **2009**, *113*, 8210–8213.
19
20 (22) LeBard, D. N.; Matyushov, D. V. Protein-water electrostatics and principles of bioenergetics.
21 *Phys. Chem. Chem. Phys.* **2010**, *12*, 15335–15348.
22
23 (23) Heyden, M.; Tobias, D. J. Spatial dependence of protein-water collective hydrogen-bond dy-
24 namics. *Phys. Rev. Lett.* **2013**, *111*, 218101.
25
26 (24) Bellissent-Funel, M.-C.; Hassanali, A.; Havenith, M.; Henchman, R.; Pohl, P.; Sterpone, F.;
27 van der Spoel, D.; Xu, Y.; García, A. E. Water determines the structure and dynamics of
28 proteins. *Chem. Rev.* **2016**, *116*, 7673–7697.
29
30 (25) Martin, D. R.; Matyushov, D. V. Solvent-renormalized dissipative electro-elastic network
31 model of hydrated proteins. *J. Chem. Phys.* **2012**, *137*, 165101.
32
33 (26) Martin, D. R.; Matyushov, D. V. Why are vibrational lines narrow in proteins? *J. Phys. Chem.*
34 *Lett.* **2020**, *11*, 5932–5937.
35
36
37
38
39
40
41
42
43
44
45
46
47
48
49
50
51
52
53
54
55
56
57
58
59
60

(27) Fried, S. D.; Boxer, S. G. Electric fields and enzyme catalysis. *Ann. Rev. Biochem.* **2017**, *86*, 387–415.

(28) Young, M. E.; Carroad, P. A.; Bell, R. L. Estimation of diffusion coefficients of proteins. *Biotech. Bioeng.* **1980**, *22*, 947–955.

(29) Gitlin, I.; Carbeck, J. D.; Whitesides, G. M. Why are proteins charged? Networks of charge-charge interactions in proteins measured by charge ladders and capillary electrophoresis. *Ang. Chem.* **2006**, *45*, 3022.

(30) Carbeck, J. D.; Negin, R. S. Measuring the size and charge of proteins using protein charge ladders, capillary electrophoresis, and electrokinetic models of colloids. *J. Am. Chem. Soc.* **2001**, *123*, 1252–1253.

(31) Zwanzig, R. *Nonequilibrium statistical mechanics*; Oxford University Press: Oxford, 2001.

(32) Balucani, U.; Zoppi, M. *Dynamics of the liquid phase*; Oxford Science Publications: Oxford, 1994.

(33) Kumar, P. V.; Maroncelli, M. The non-separability of “dielectric” and “mechanical” friction in molecular systems: A simulation study. *J. Chem. Phys.* **2000**, *112*, 5370–5381.

(34) Baiz, C. R.; Błasiak, B.; Bredenbeck, J.; Cho, M.; Choi, J.-H.; Corcelli, S. A.; Dijkstra, A. G.; Feng, C.-J.; Garrett-Roe, S.; Ge, N.-H. et al. Vibrational spectroscopic map, vibrational spectroscopy, and intermolecular interaction. *Chem. Rev.* **2020**, *120*, 7152–7218.

(35) Ma, C.; Malessa, A.; Boersma, A. J.; Liu, K.; Herrmann, A. Supercharged proteins and polypeptides. *Adv. Mater.* **2020**, *32*, 1905309.

(36) McNaughton, B. R.; Cronican, J. J.; Thompson, D. B.; Liu, D. R. Mammalian cell penetration, siRNA transfection, and DNA transfection by supercharged proteins. *Proc. Natl. Acad. Sci. USA* **2009**, *106*, 6111–6116.

1
2
3 (37) Balabai, N.; Sukharevsky, A.; Read, I.; Strazisar, B.; Kurnikova, M. G.; Hartman, R. S.;
4 Coalson, R. D.; Waldeck, D. H. Rotational diffusion of organic solutes: the role of dielectric
5 friction in polar solvents and electrolyte solutions. *J. Molec. Liq.* **1998**, *77*, 37–60.
6
7
8 (38) Berne, B. J.; Pecora, R. *Dynamic light scattering*; Dover Publications, Inc.: Mineola, N.Y.,
9 2000.
10
11 (39) Wong, V.; Case, D. A. Evaluating rotational diffusion from protein MD simulations. *J. Phys.*
12
13 *Chem. B* **2008**, *112*, 6013–6024.
14
15 (40) Till, M. S.; Ullmann, G. M. McVol - A program for calculating protein volumes and identify-
16 ing cavities by a Monte Carlo algorithm. *J. Mol. Mod.* **2010**, *16*, 419.
17
18 (41) Edmond, K. V.; Elsesser, M. T.; Hunter, G. L.; Pine, D. J.; Weeks, E. R. Decoupling of rota-
19 tional and translational diffusion in supercooled colloidal fluids. *Proc. Natl. Acad. Sci. USA*
20
21 **2012**, *109*, 17891–17896.
22
23
24 (42) Roos, M.; Ott, M.; Hofmann, M.; Link, S.; Rössler, E.; Balbach, J.; Krushelnitsky, A.; Saal-
25 wächter, K. Coupling and decoupling of rotational and translational diffusion of proteins un-
26 der crowding conditions. *J. Am. Chem. Soc.* **2016**, *138*, 10365–10372.
27
28
29 (43) Haridasan, N.; Kannam, S. K.; Mogurampelly, S.; Sathian, S. P. Rotational diffusion of pro-
30 teins in nanochannels. *J. Phys. Chem. B* **2019**, *123*, 4825–4832.
31
32
33 (44) Martin, D. R.; Fioretto, D.; Matyushov, D. V. Depolarized light scattering and dielectric re-
34 sponse of a peptide dissolved in water. *J. Chem. Phys.* **2014**, *140*, 035101.
35
36
37
38
39
40
41
42
43
44
45
46
47
48
49
50
51
52
53
54
55
56
57
58
59
60